Geostatistical Analysis of CPT-UVIF Data for Development of a Site Conceptual Model

Amir H Hosseini, PhD candidate, Department of Civil and Environmental Engineering, University of Alberta, Edmonton, AB, Canada

Kevin W Biggar, Professor, Department of Civil and Environmental Engineering, University of Alberta, Edmonton, AB, Canada

Clayton V Deutsch, Professor, Department of Civil and Environmental Engineering, University of Alberta, Edmonton, AB, Canada

Carl A Mendoza, Associate Professor, Department of Earth and Atmospheric Sciences, University of Alberta, Edmonton, AB, Canada

Abstract

Cone Penetration Testing (CPT) provides detailed information about soil type and associated design parameters. Ultra Violet Induced Fluorescence Cone Penetration Testing (CPT-UVIF) has been used frequently in environmental site characterization to delineate subsurface stratification as well as lateral and vertical hydrocarbon distribution. The information collected during site investigation provides a basis for further site investigations and for evaluating the applicability of various remedial techniques. This information, however, is incomplete which translates to uncertainty in bounding the problem and increases the risk of regulatory non-compliance or excess costs. To attain a better understanding of geological structure and NAPL distribution, this uncertainty should be assessed and quantified. Using geostatistical techniques, models of uncertainty for geological structure and non-aqueous phase liquid (NAPL) distribution have been developed for a hydrocarbon impacted site. In conjunction with CPT data analysis techniques, the Sequential Indicator Simulation (SIS) approach has been used to determine the site lithology and extent of contaminant source zone. The original spatial continuity is captured and trends are reproduced. Based on the models of uncertainty for geological structure and contaminant source zone and their association, a conceptual model can be developed for the site. Results of this work will ultimately provide a framework for subsequent numerical modeling of natural attenuation of petroleum hydrocarbons at the site.

Introduction

Risk and uncertainty are characteristics of the ground and never can be eliminated, but can be quantified. Even with combination of most extensive site investigation schemes, only a small portion of ground can be fully characterized. In every geo-environmental engineering project, there are a number of important objectives for site investigations. These include nature and sequence of the subsurface strata, groundwater conditions, physical properties of subsurface strata (e.g. hydraulic conductivity), and distribution and composition of contaminants.

Cone Penetration Testing (CPT) has two main applications in the site investigation processes associated with geo-environmental applications. One is to determine sub-surface stratigraphy and identify materials present; and the other is to estimate geo-engineering parameters (Lunne, Robertson and Powell 1997). In geo-engineering practice, CPT has been used frequently for soil profiling and classification. There is an extensive experience in relating CPT results to soil type. Experience has shown that typically the cone penetration resistance is high in sands and low in clays and the dimensionless ratio between sleeve-friction and cone resistance (friction ratio) is low in sands and high in clays. CPT data provide a repeatable index of the aggregate behavior of the in-situ soil in the immediate area of the probe. The prediction of soil type based on CPT results is usually referred to as soil behavior type (Robertson 1998). One of the most commonly used CPT soil behavior type (SBT) charts is the one suggested by Robertson et. al. (Robertson et al. 1986). Figure 1(a) shows this soil behavior type classification chart.

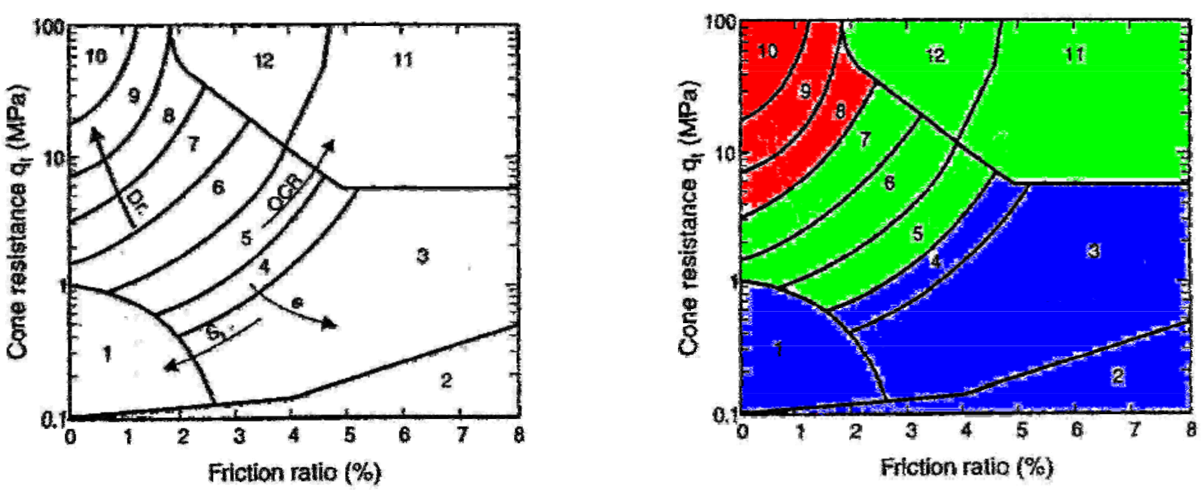

Figure 1: (left) non-normalized soil behavior type classification chart (Robertson et al. 1986) and (right) grouping SBTs into three categories based on their estimated hydraulic conductivities.

SBT classification charts give an estimate of hydraulic conductivity of soils. Although these estimates are approximate, they can provide a guide to variations of hydraulic conductivity at sampling locations. In order to use the SBT charts in subsequent geostatistical modeling and to prevent the large-scale geological features from being masked by unrealistic short-scale variations, all SBTs are grouped into three different categories. These categories will be used as inputs for Sequential Indicator Simulation (SIS) technique to generate: (1) equi-probable realizations of geological structure for use in reproduction of hydraulic conductivity, and (2) probability maps showing continuity of geological strata at the site.

Delineation of source zone is a very important step in environmental site characterization for sites impacted by petroleum hydrocarbons (PHCs). Non-aqueous phase liquids (NAPLs) composed of aromatic hydrocarbons can be successfully detected by fluorescence. Commercially available Ultra Violet Induced Fluorescence Cone Penetrometer (CPT-UVIF) is a standard CPT cone combined with a detecting tool for ultraviolet induced fluorescence. The UVIF module consists of a high intensity UVIF light projected into the surrounding soil and a photo multiplier tube sensor to record fluorescence. The currently available CPT-based fluorescence systems are typically restricted to a single wavelength excitation source, each demonstrating specific advantages and disadvantages with respect to detection capabilities for particular fluorophores (Kram et al. 2004). According to CCME criteria, the wavelength used in this study is corresponding to C34 to C50 (F4) fractions (Canadian Council of Ministers of the Environment 2001).

In previous studies, the magnitude of fluorescence was directly related to the relative concentration of aromatic PHCs present in the soil (Armstrong, Deutsch and Biggar 2004). Using indicator simulation techniques, in this study, a newer approach is taken by development of a model of absence/presence for NAPL contamination to remove effects of aggregate size on UVIF recordings. This approach introduces a risk-based framework for contaminant source distribution. Continuity of hydrocarbon impacted zones is better reproduced. Effects of other controlling factors such as geological structure and stratification are also added to the model to improve the model of source zone.

This study was performed as part of a larger research project termed CORONA (Consortium for Research on Natural Attenuation) to assess Monitored Natural Attenuation as a cost-effective scheme for remediation of upstream oil and gas sites (exploration and production industry). The findings of this study are used in subsequent fate and transport modeling to develop a risk-based approach to prediction of Natural Attenuation at upstream oil and gas sites.

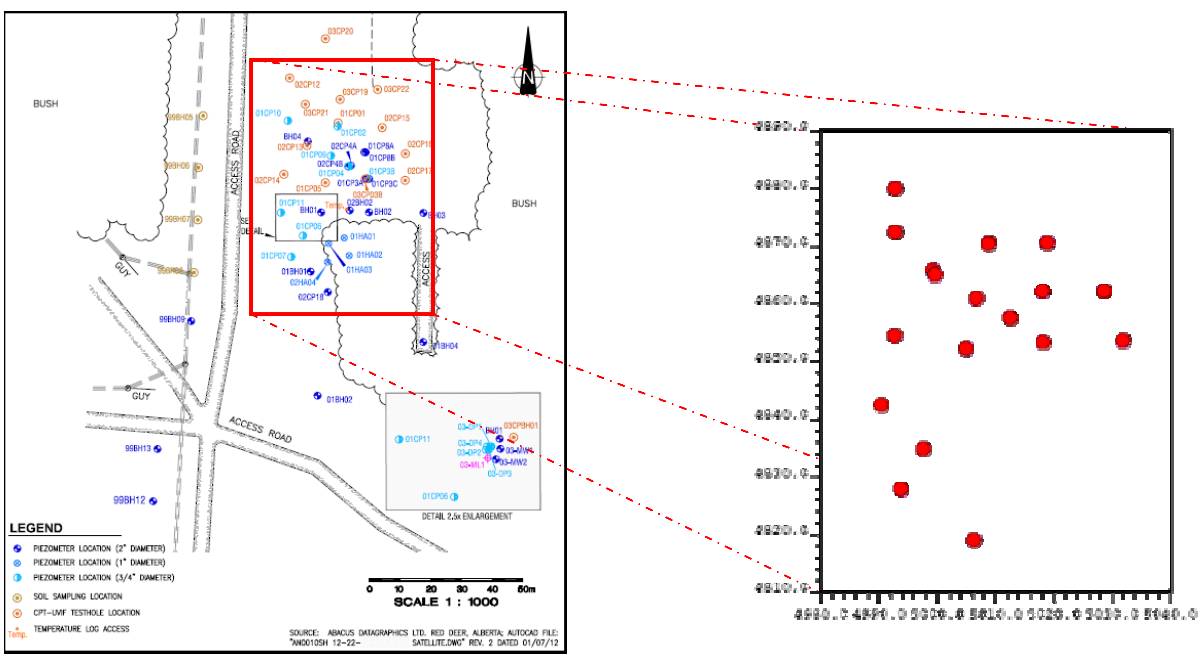

Figure 2: (left) locations of boreholes, monitoring wells and CPT-UVIF holes; and (right) Locations of 18 CPT-UVIF holes as well as domain for geostatistical study.

Hydrocarbon Impacted Site

The study site is a former flare pit site located in west-central Alberta close to the town of swan hills. Solid stem auger method was used for initial drilling. Soil logs showed heterogeneous distribution of clay, silt and sandy units (Armstrong, Deutsch and Biggar 2004). The location of the former flare pit is roughly known to be in the north of the site. The exact limits, however, are not known. The site slopes from north to south. A few years ago, heavily contaminated soil at the north of the site was excavated to depths of 4 – 5 m and backfilled with clean soil. According to initial soil sampling analysis, free-phase hydrocarbons (NAPLs) were suspected to remain at the site. However, its presence had not been confirmed in the four nearest monitoring wells. The site was characterized through logging and sampling 16 boreholes drilled using the solid stem auger method to approximately 5 m below ground surface. Based on these data, 18 CPT-UVIF holes were advanced in two phases. The holes ranged in depth from 4 to 11 m below ground surface (Armstrong, Deutsch and Biggar 2004). Figure 2 shows the locations of sampling points, monitoring wells as well as CPT-UVIF holes and geostatistical modeling domain. The modeling domain is 60 m in east-west direction, 80 m in north-south direction, and 16 m in depth.

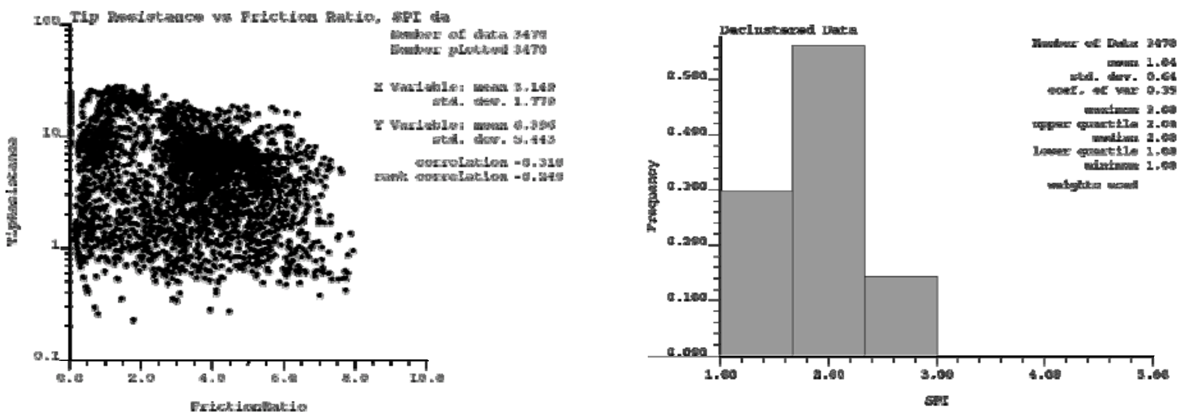

Figure 3: (left) Cone resistance vs. friction ratio values for 18 CPT cones; and (right) histogram of declustered soil type data.

Geostatistical analysis for geological structure

The decision of which data should be pooled together for subsequent analysis is the "decision of stationarity" (Deutsch 2002). In other words, the decision of stationarity implies that mean (or prior probability) is independent from location (Goovaerts 1997). The decision of stationarity may be revised based on further steps of data analysis. For instance, while observing a bimodal (two peaks) histogram for data, one might want to consider separating the data into two classes with distinct statistical and geological properties (Deutsch 2002). In fact, separating the data set into more homogenous geologic and hydrogeologic zones improves the accuracy of the estimates. Indicator kriging offers an alternate method that is more appropriate for data showing non-stationarity in its basic statistics. Using indicator kriging to identify various 'soil types' or geological regions with distinct statistical and geological features enhances data homogeneity within sub-regions and makes the decision of stationarity more appropriate (Rouhani and ASTM Committee D-18 on Soil and Rock 1996).

For every hole, CPT-UVIF tool records cone resistance, sleeve friction, pore pressure and ultraviolet induced fluorescence at approximately every 5 cm. Plotting cone resistance vs. friction ratio for every data location, one can observe distribution of data throughout the site and can identify different soil types. Using the plotted data (figure 3) and SBT chart (figure 1), geological structure can be grouped into three sub-regions comprising soils with distinct statistical and hydrogeological features. Configuration of sampling points is clustered at the site which means all the data are not equally representative in summary statistics and must be weighted. Cell declustering is performed in this study using *declus* program in GSLIB (Deutsch and Journel 1998). The resulted histogram of soil type data is displayed in figure 3. According to Robertson (Robertson 1998), each of these three soil types has an estimated range of hydraulic conductivities. Soil type one, with a frequency of 29.5 %, has hydraulic conductivity values approximately ranging from 1×10^{-11} m/s to 1×10^{-8} m/s. For soil type two, having a frequency of 55 % and covering majority of the site, hydraulic conductivity values approximately range from 1×10^{-9} m/s to 1×10^{-5} m/s. Soil type three, with a frequency of 15.5 %, has hydraulic conductivity values approximately ranging from 1×10^{-5} m/s to 1×10^{-2} m/s.

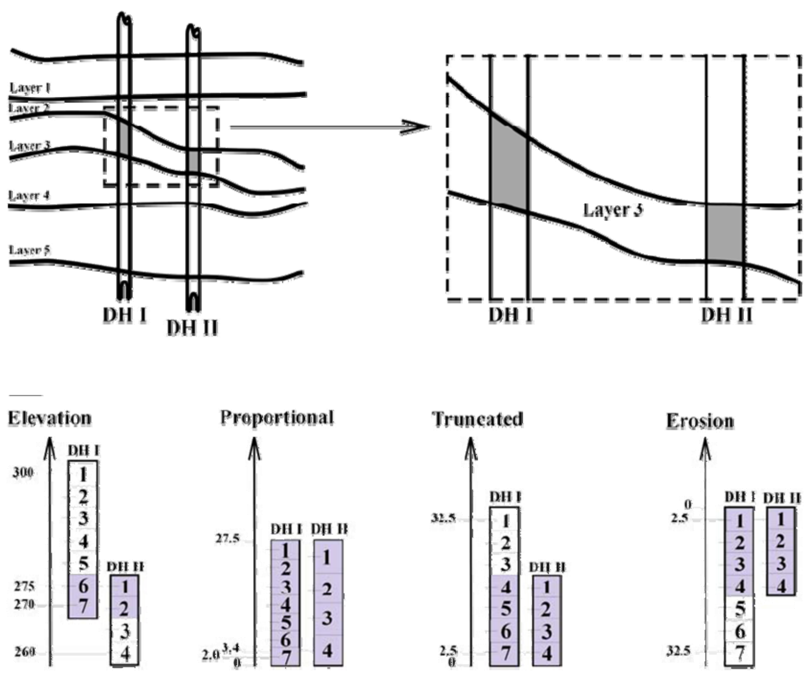

Figure 4: (top) A five-layer geological structure, samples taken from layer 3; and (bottom) Various coordinate transformation scenarios are calculated and shown. The shaded composites represent horizontal variogram calculation pairs (McLennan, 2004)

Identifying directions of geological continuity

In presence of stratification and layering in geological structure, the decision of stationarity may no longer be appropriate. Even though all data have been already splitted into three groups based on their statistical and geological features, it is still needed to delineate right directions of geological continuity and detect any inclination in geological units. This requirement is a direct result of two important facts: (1) in geostatistical analysis the model is constructed on a Cartesian grid; and (2) the bounding surfaces between the layers correspond to a specific geologic time that separates two different periods of deposition or a period of erosion or consolidation followed by deposition, and are not often horizontal (Deutsch 2002). Thus, prior to calculation of directional variograms for different categories, a vertical coordinate transformation must be performed, considering various common deposition-erosion or consolidation-erosion scenarios.

As a standard practice, horizontal variograms are calculated after each coordinate transformation and the scenario showing highest degree of correlation is retained and the rest of the geostatistical modeling is done in the new coordinate system. The final results will be ultimately back-transformed to original coordinate system. Four different deposition-erosion scenarios are schematically shown in figure 4. For the present site, the original vertical coordinates happened to show highest degree of continuity (elevation scenario).

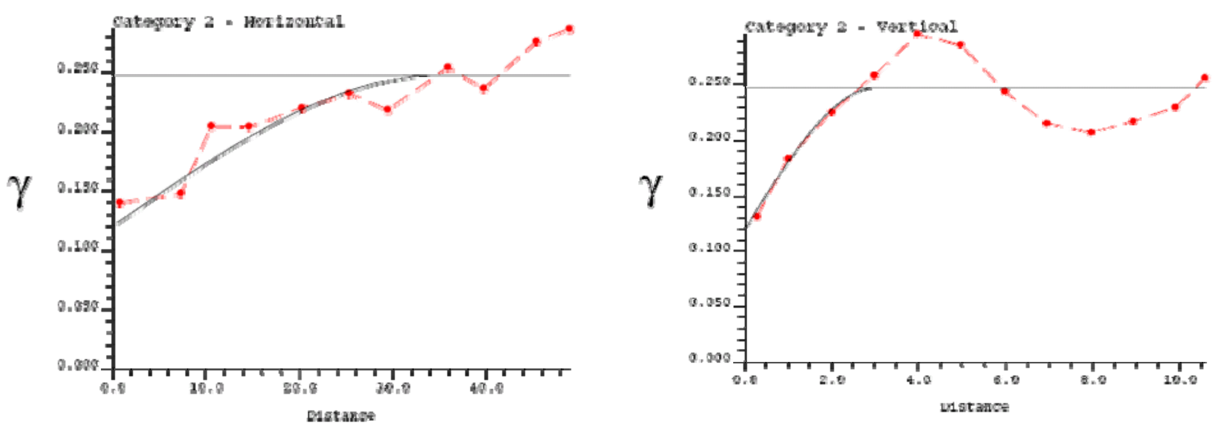

Figure 5: dashed lines and solid lines show calculated (experimental) and modeled variograms, respectively; (left) Horizontal variogram for soil type 2; (right) Vertical variogram for soil type 2

Modeling indicator variograms

Unlike Gaussian techniques, indicator formalism is capable of incorporating different spatial continuity for different categories. Indicator variograms are calculated for each category using the available site-specific data. The data used in calculation of indicator variograms are the data which have been transformed to soil type indices (1's, 2's and 3's for three different soil types). Figure 5 shows calculated and modeled variograms in horizontal and vertical directions for soil type 2. Similar directional variograms calculated and modelled for soil types 1 and 3.Sills of all variograms are calculated by $p(1-p)$ where $p = F(z_k)$ is the global proportion of indicator variable before declustering. Range of a variogram is horizontal distance between the origin of the variogram and the point in which variogram reaches to the sill. As the range becomes larger, a smaller variability is observed in nearby data. As comparing the ranges of vertical and horizontal variograms in figure 5, the effect of stratification can be clearly observed. It should be noted that spherical structure has been used in modeling variograms for all three soil types. Variogram calculation and modeling has be performed using GSLIB (Deutsch and Journel 1998).

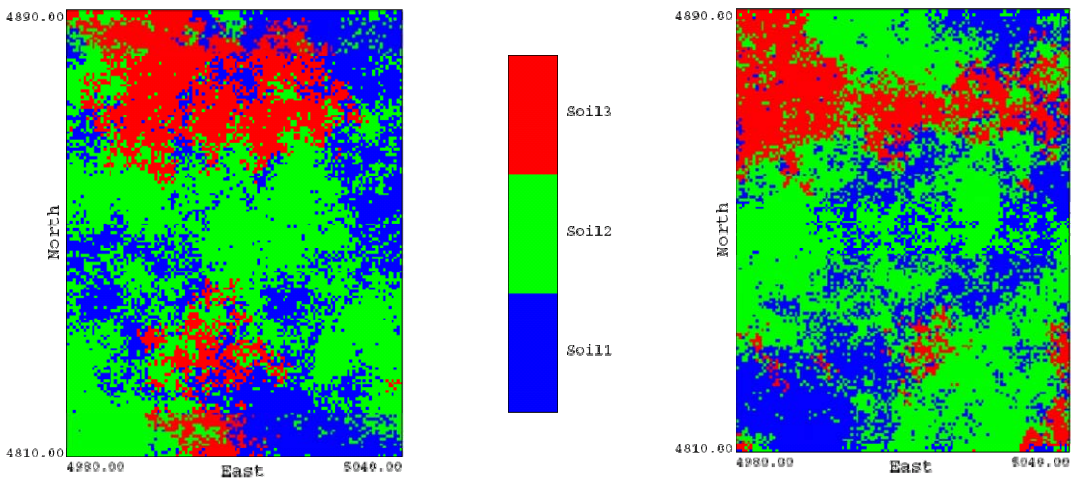

Figure 6: Two equi-probable realizations showing distribution of three soil types throughout the site. Theses realizations honor the input data (site-specific samples) and input statistics very well. The above slices are planar views taken at mid-height of the modeling domain.

Indicator kriging and Sequential Indicator Simulation (SIS)

Indicator kriging (IK) (Deutsch and Journel 1998) and simulation are used to directly estimate the distribution of uncertainty in the categorical variables. As the first step in indicator formalism, site-specific data at every data location is coded as indicator values (Deutsch 2002):

$$i(\mathbf{u}_\alpha; z_k) = Prob\{\text{soil type } k \text{ being present}\}$$
$$= \begin{cases} 1, & \text{if soil type } k \text{ is present at } \mathbf{u}_\alpha \\ 0, & \text{otherwise} \end{cases} \quad (1)$$

The stationarity prior probabilities of different soil types ($p(k),\ k = 1,\ 2,\ 3$) have been determined using histogram of declustered data (figure 3).Based on figure 3, $p(1) = 0.295$, $p(1) = 0.55$, and $p(1) = 0.155$. According to (1), residual data can be written as:

$$Y(\mathbf{u}_\alpha; z_k) = i(\mathbf{u}_\alpha; k) - p(k), \quad \alpha = 1, 2, \ldots, \text{n}, \quad k = 1, 2, 3 \quad (2)$$

According to Deutsch (2002), kriging of these residual data is used to derive the probability of occurrence of each soil type at every unsampled location. Thus, the model of uncertainty at every unsampled location **u** will be:

$$p_{IK}(\mathbf{u};k) = \sum_{\alpha=1}^{n} \lambda_\alpha(k).[i(\mathbf{u}_\alpha;k) - p(k)] + p(k), \qquad k = 1, 2, 3 \tag{3}$$

where subscript *IK* denotes Indicator Kriging, λ_α's are weighting factors which account for closeness to data points as well as overall uncertainty in the domain and redundancy in nearby data. These weighting factors are calculated using the Simple Kriging (SK) system of equations. Variogram measures of correlation are used in constructing the SK system of equations.

The estimated probabilities must be non-negative and sum to one. As these requirements are not often fully satisfied by indicator kriging (IK) with categorical variables, a post-correction procedure is often performed.

Sequential Indicator Simulation (SIS) (Deutsch and Journel 1998) is a Monte Carlo simulation technique built on Indicator Kriging (IK) explained above. In order to populate the whole modeling domain with simulated values, grid nodes are visited sequentially in a random path. At each grid node the following procedure is repeated (Deutsch 2002): (1) searching for nearby data and previously simulated values, (2) performing IK to build a distribution of uncertainty, and (3) drawing a simulated value from the distribution of uncertainty.

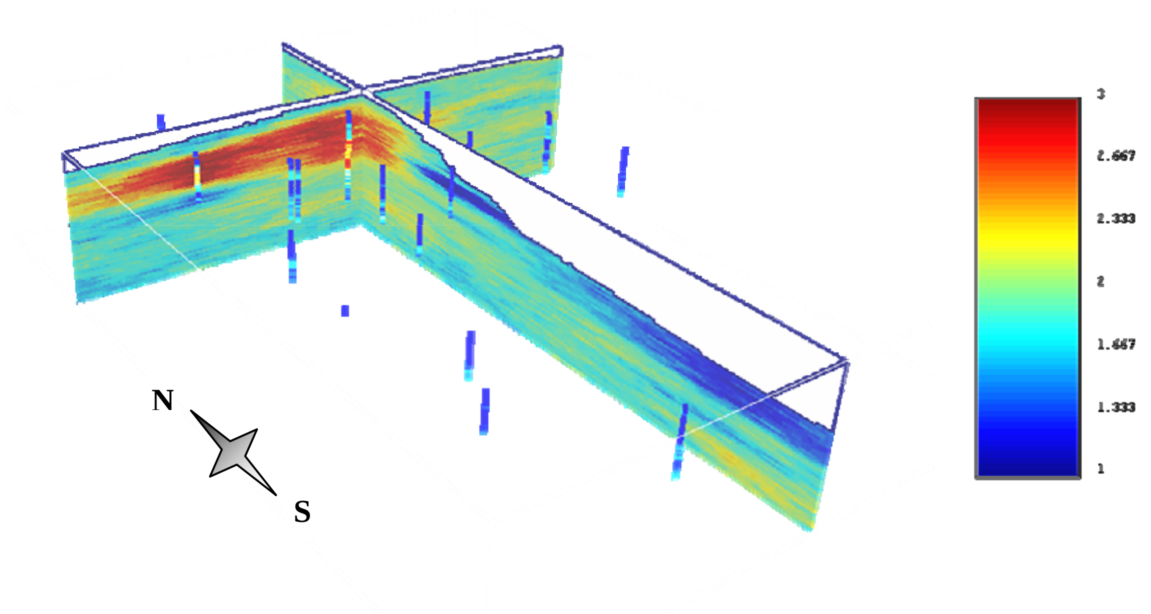

Figure 7: Two cross-sectional views of the 3D likelihood map for soil types. There is a large sandy layer (soil type 3) on northwest of the site. While, south of the site is mainly comprised of lower permeability units (soil types 1 and 2). Topography has been also displayed. Site generally slopes from the north to the south.

Analyzing and post-processing of the results

As a result of Sequential Indicator Simulation, a large number of equi-probabale soil-type realizations are generated (figure 6). These realizations reproduce the input data equally well. There are a number of checks which have been done to validate the model as a fairly good representative for the unknown reality: (1) reproduction of input statistics such as histogram and variograms, (2) honoring input data, (3) consistency with the available information about geology of the site, as well as checking the model predictions by (4) closeness of estimated probabilities to the true soil types (both for CPT cones as well as borehole logs), and (5) accuracy of the local probabilities.

As observed in figure 6, SIS realizations are often show unrealistic short-scale variations. Using 'maximum a-posteriori selection' technique (MAPS), (Deutsch and Journel 1998), the realizations are cleaned from these short-scale variations and slight deviations from global proportions (order relations problem) are controlled and fixed.

The cleaned realizations are then used in (1) development of a 3D likelihood map for 'Soil Type' in the modeling domain, (2) stochastic simulation of hydraulic conductivity throughout the site, and (3) development of a prior probability map for NAPL contamination.

Figure 7 shows two cross-sectional views of the 3D likelihood map for soil type as well as CPT cones. The magnitude of cone resistance is shown on the wells. As shown in the cross-sectional views, there is a large sandy layer (soil type 3) in depths from 1 m to 7 m extended to the northwest of the site. While, south of the site is mainly comprised of lower permeability units (soil types 1 and 2). Topography has been also displayed. Site generally slopes from the north to the south. Very high likelihood for presence of a large sandy layer (in specific depths) on the northwest of the site should be considered in design of any remediation scheme. South of the site (especially in smaller depths) is less likely to be a good pathway for contaminants to further downstream. Deeper areas on the south, however, are more likely to be good pathways for transport of contaminants. It should be brought into attention that, based on independent site observations (borehole logs), the results of the model show the continuity and extent of geological features very well.

The generated soil-type realizations are also used in reproduction of hydraulic conductivities for subsequent use in fate and transport modeling. When plotting histogram of sparse hydraulic conductivity data from the site, it is observed to be highly skewed and has a tri-modal shape. Assigning separate Gaussian distributions of hydraulic conductivity (with different means and variances) to each of the three soil types ensures reproduction of the tri-modal shape for hydraulic conductivity distribution in every realization. These equi-probable realizations may then be used as inputs for stochastic (Monte Carlo) simulation of fate and transport for dissolved contaminants.

The soil-type realizations are also used in development of a 3D prior probability map for presence of free-phase product (NAPL) at the site. Later in this paper, correlation between soil type and presence of NAPL is discussed and the prior probability map will be developed.

Geostatistical analysis for contaminant source zone

As stated before, UVIF data may be unrealistically affected by aggregate size. This introduces an artifact in distribution of free-phase product, if one directly relates UVIF data to NAPL concentrations. In order to avoid this artifact, a threshold is introduced in this study and a model of presence/absence is developed for NAPL contaminants. Results of this modeling effort introduce a risk-based framework for contamination.

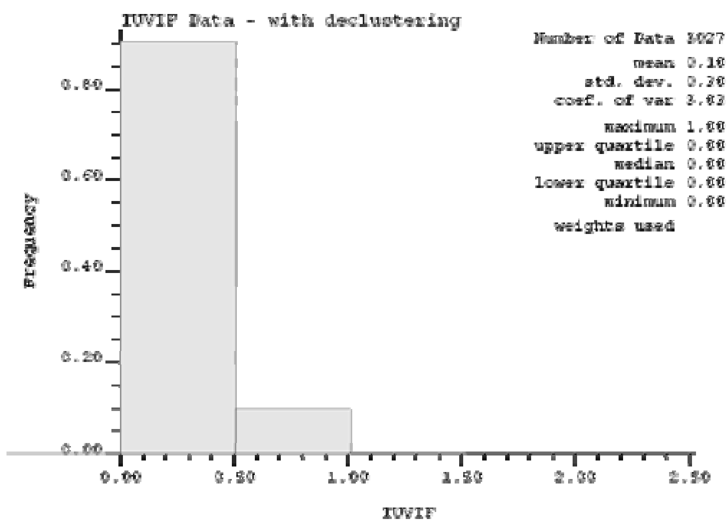

Figure 8: (left) Histogram of declustered binary TUVIF data for NAPL contamination

First, a model of contaminant source zone is developed solely based on available UVIF data. This model, however, does not show the lateral spread of contaminant plume appropriately. In order for the NAPL plume to conform important geological features, the site-specific correlation between presence of NAPL and type of soil is studied and incorporated into the model as secondary information. The results of this 'co-simulation' are then compared to those of the original model of contaminant source zone.

Modeling contaminant source zone using Truncated UVIF (TUVIF) data

The recorded UVIF data is in units of volts. For this site, the minimum and maximum recorded values for UVIF are 0.4 and 8.79 volts, respectively. After a series of sensitivity analyses, a threshold of 1.2 has been selected to truncate the data and develop a binary absence/presence model. Selection of this threshold is an important step and it is still subject to further research. It should be kept in mind that this threshold must be chosen in a way to prevent carbon content of the soil from being identified as NAPL contamination. On the other hand, it must be selected in a way that truncated data does not miss any free-phase product present in the soil.

Figure 8 shows histogram of binary absence/presence data. According to Figure 8, 10 percent of the data are identified as contaminated. Assuming stationarity in the data, this means 10 percent of the whole site is considered contaminated.

Figure 9 shows directional indicator variograms for TUVIF data. The ranges of variograms in binary models are related to the perimeter of the objects (or plumes in this study) in a 3D space (Monestiez, Allard and Froidevaux 2001). This relationship may be used to obtain an estimate of average sizes of plumes.

Indicator kriging (IK) and sequential indicator simulation (SIS) are performed after variogram modeling. According to equation (3), indicator kriging gives an estimate of local uncertainty at every location. GSLIB (Deutsch and Journel 1998) was used to perform indicator kriging and SIS. SIS procedure for modeling the source zone is the same as procedure for the model of soil types presented above.

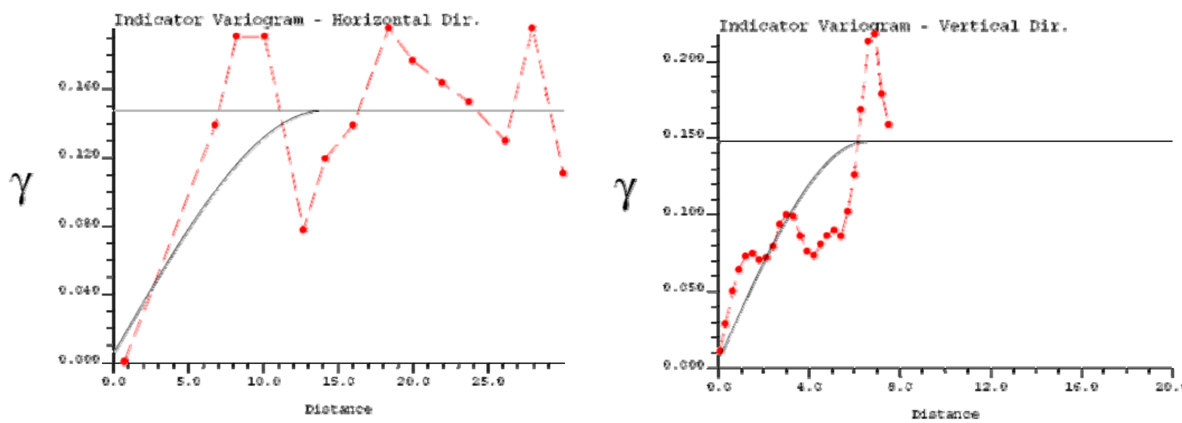

Figure 9: dashed lines and solid lines show experimental and modeled variograms, respectively; (left) Horizontal variogram and (right) Vertical variogram for model of contamination

A large number of equi-probable realizations will be generated. These realizations are used in development of a 3D probability map for contamination. Defining a series of probability thresholds, the probability map can be visualized in a risk-based format. Figure 10 shows planar views of a series of 3D risk maps. Each of these risk maps shows extent of NAPL plume for a certain degree of associated risk. For instance, for the map with an associated risk of 90 percent, there is a 90 percent or more probability for the soil in the marked areas to be contaminated. Figure 11 shows lateral and vertical extent of NAPL plume with an associated risk of 30 percent or more. As shown in figure 11, the plume seems to have a bulky shape and does not follow stratification patterns observed in soil structure (figures 7). Based on this, it is required to some how incorporate the model of geological continuity and soil structure into the model of NAPL plume. As observed later in this study, the plume will be unrealistically small and bulky, if stratification is not taken into account.

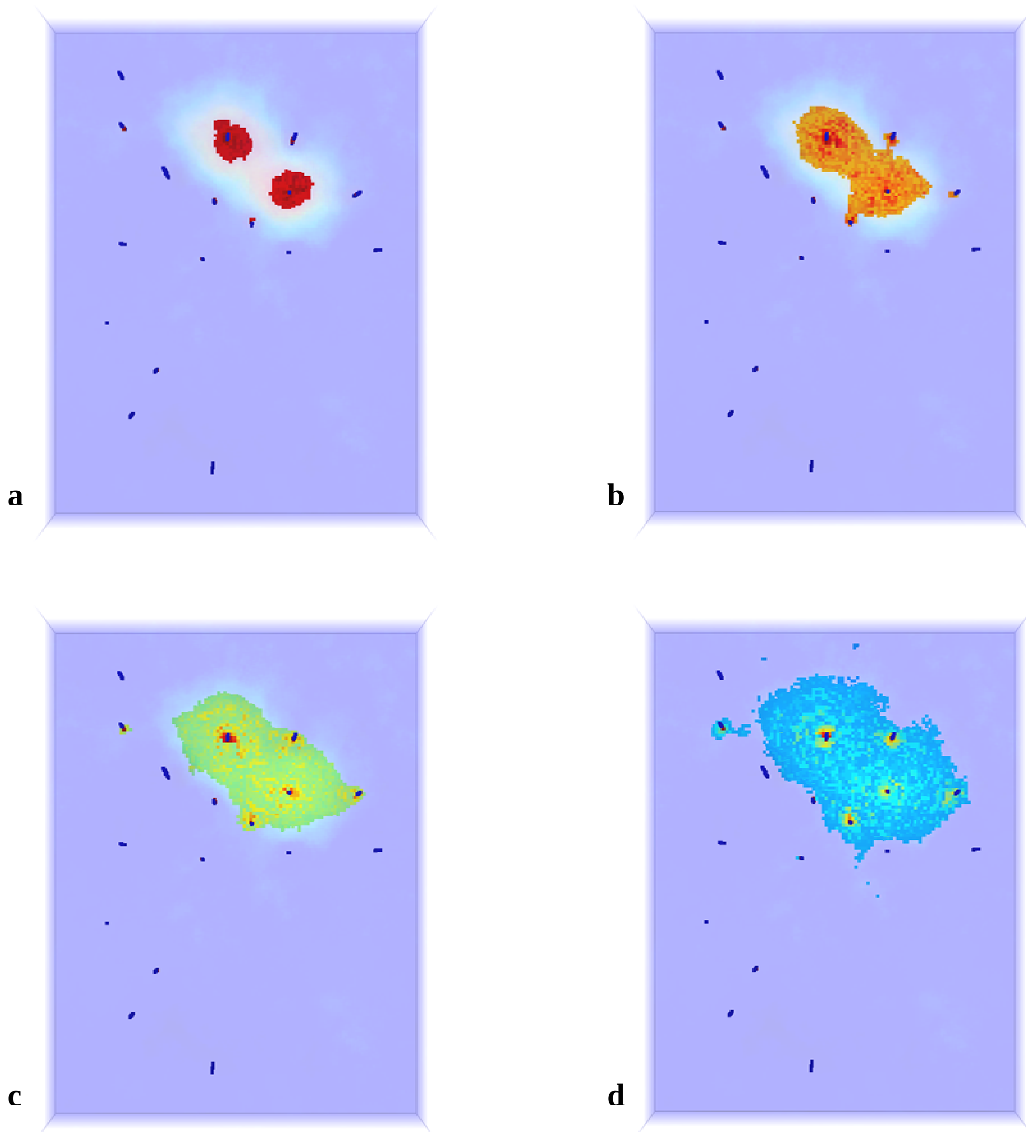

Figure 10: Planar views of risk maps showing extent of NAPL plume for different levels of risk: (a) 90 percent, (b) 70 percent, (c) 50 percent, and (d) 30 percent.

Modeling contaminant source zone using TUVIF data and model of geological structure as secondary information

The model of geological structure can be successfully used as secondary information to improve the model of source zone. There are a number of reasons for this:

1. There is an evident correlation between presence of free phase product (NAPL) and grain size of aggregates: The larger grain sizes and pore spaces, the more likely presence of free phase product;

2. More information is often available about geological structure. Moreover, obtaining information about geology of the site is often much cheaper, easier and more reliable as compared to gathering information about contaminant distribution;
3. Unlike contaminant distribution, geological structure often shows higher ranges of correlation and larger distances of continuity. This can be observed in figures 5 and 9. In fact, direction of continuity and inclination of strata play important roles in prediction of NAPL distribution in subsurface.

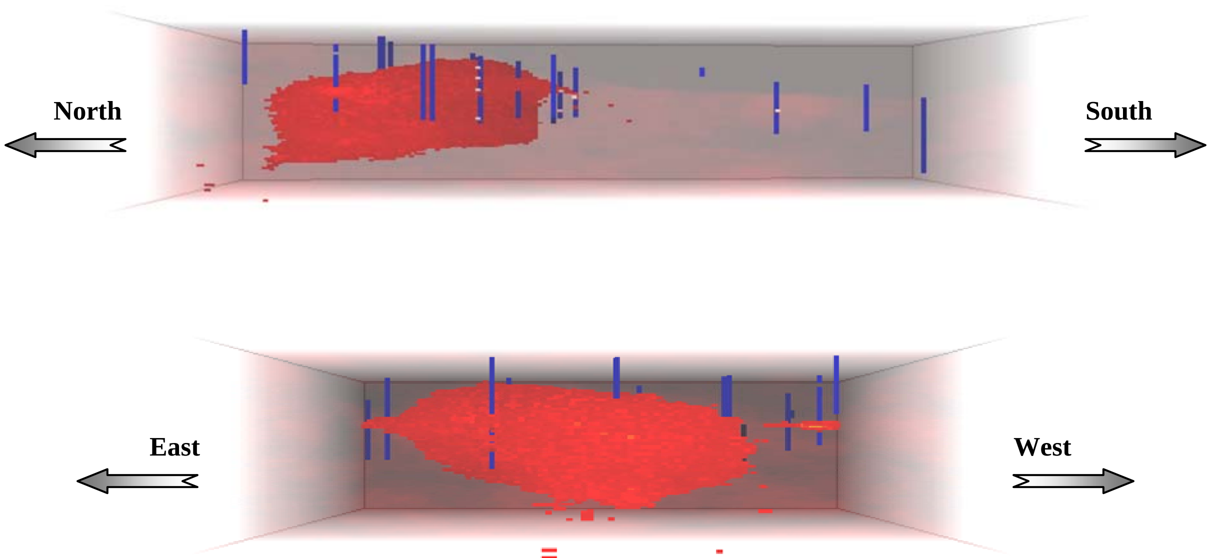

Figure 11: Cross-sectional views of risk maps showing vertical and lateral extent of NAPL plume for a risk of 30 percent.

To incorporate the geological model in the model of source zone as secondary information, first of all, correlation between site-specific soil type data and TUVIF data must be determined. Table 1 shows this correlation. According to the table, whenever soil type 3 is observed at a location, there is a probability of 14.67 percent for that location to be contaminated. This probability is 8.95 for soil type 2 and 8.68 for soil type 1. The cokriging estimate is written by:

$$\hat{i}(\mathbf{u};k)=\sum_{\alpha=1}^{n}\lambda_\alpha \cdot i(\mathbf{u}_\alpha;k)+\left[1-\sum_{\alpha=1}^{n}\lambda_\alpha\right]\cdot p(k|ai(\mathbf{u})) \tag{4}$$

in which, $\hat{i}(\mathbf{u}_\alpha;k)$ is probability of presence of NAPL at location $\mathbf{u}$, $i(\mathbf{u}_\alpha;k)$ is indicator data for presence or absence of NAPL (a binary variable) and is defined in a way similar to equation (1), λ_α's are weighting factors which account for closeness to data points as well as overall uncertainty in the domain and redundancy in nearby data. The term $p(k|ai(\mathbf{u}))$ represents prior probability for presence of NAPL. This is a location-dependent attribute and is calculated by assigning the correlation factors summarized in table 1 to a large number of equi-probable soil-type realizations (figure 6). According to equation (4), at every location of the modeling domain, $p(k|ai(\mathbf{u}))$ receives a higher weight when there are smaller number of data in close proximity of location being estimated and vice versa.

	Presence (%)	***Absence (%)***
Soil Type 1	**8.68**	**91.32**
Soil Type 2	**8.95**	**91.05**
Soil Type 3	**14.67**	**85.33**
Weighted Average	**10**	**90**

Table 1: Correlation factors between soil type data and presence of contamination

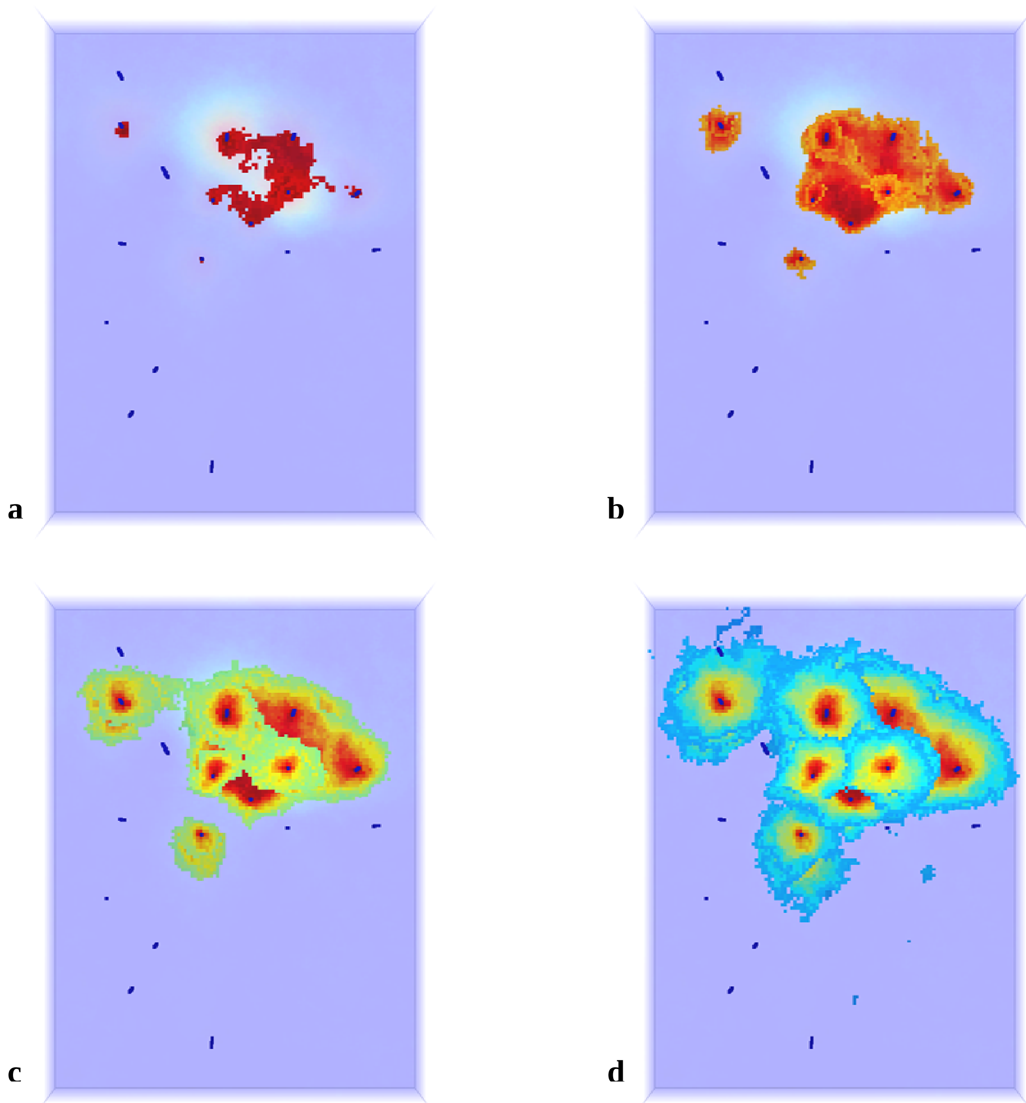

Figure 12: Planar views of risk maps showing extent of NAPL plume, resulted from **cosimulation** for different levels of risk: (a) 90 percent, (b) 70 percent, (c) 50 percent, and (d) 30 percent.

The results of the co-simulation are shown in figures 12 and 13. Comparing figure 13 to figure 11, one can evidently observe capability of the co-simulation in modeling lateral continuity of NAPL plumes. Also, comparing figure 12 to figure 10 shows if the geological continuity is not incorporated into the model of source zone, size and lateral extent of the plume may be significantly under-estimated.

The risk maps, developed for contaminant source zone, clearly show extent of contamination for different risk levels. These are valuable tools for sample optimization purposes, whenever additional sampling is required. Including other controlling factors, such as groundwater fluctuations, as secondary variables can also enhance prediction capability. The risk maps and likelihood maps can also be used in conjunction with other design factors to increase effectiveness of active remediation schemes to reduce the overall cost of remediation projects.

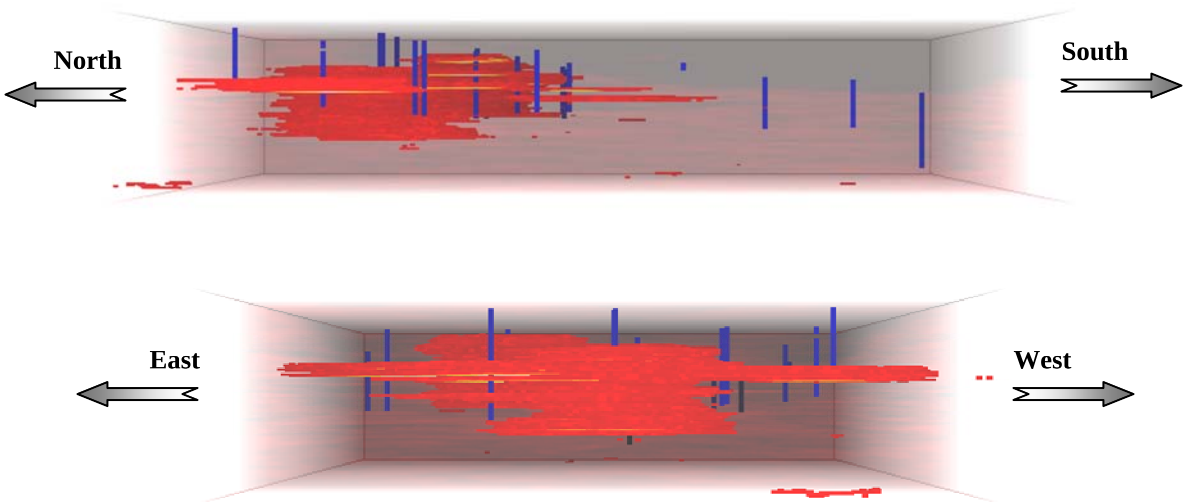

Figure 13: Cross-sectional views of risk maps, resulted from **cosimulation**, showing vertical and lateral extent of NAPL plume for a risk of 30 percent.

Conclusions

Geostatistical Modeling is a powerful tool in studying geological structure by providing information about continuity of subsurface strata and location of high permeability conduits. It is also applicable in reproduction of representative hydraulic conductivity values throughout the site.

Geostatistical analysis can be used to delineate contaminant source zone and gives an estimate of plume size. The model of contaminant source zone can be successfully improved by incorporating some secondary information such as geological structure. This secondary information can be any property which is some how quantifiable. Indicating directions of maximum likelihood for contamination and lateral and vertical extent of NAPL plume, the model can be used in sampling optimization programs, when the site is subject to additional sampling.

References

Armstrong, J. E., C. V. Deutsch, and K. W. Biggar, 2004: Geostatistical Assessment of Cone Penetrometer Test Data for Contaminant Assessment Based on Ultraviolet Induced Fluorescence. *Proceeding of the 57th Canadian Geotechnical Conference and the 5th Joint CGS/IAH-CNC Groundwater Specialty Conference,* , 17.

Canadian Council of Ministers of the Environment, 2001: Reference Method for the Canada-Wide Standard for Petroleum Hydrocarbons in Soil - Tier1Method. , 44.

Deutsch, C. V., 2002: *Geostatistical Reservoir Modeling.* Oxford University Press, 376 pp.

Deutsch, C. V. and A. G. Journel, 1998: GSLIB : geostatistical software library and user's guide. , 369.

Goovaerts, P., 1997: *Geostatistics for natural resources evaluation.* Oxford University Press, 483 pp.

Kram, M. L., A. A. Keller, S. M. Massick, and L. E. Laverman, 2004: Complex NAPL site characterization using fluorescence part 1: Selection of excitation wavelength based on NAPL composition. *Soil and Sediment Contamination,* 13, 103-118.

Lunne, T., P. K. Robertson, and J. Powell, 1997: *Cone Penetration Testing in Geotechnical Practice.* Thomson Professional Publishers,

Monestiez, P., D. Allard, and R. Froidevaux, 2001: *GeoENV III : geostatistics for environmental applications : proceedings of the third European Conference on Geostatistics for Environmental Applications held in Avignon, France, November 22-24, 2000.* Vol. 11. Kluwer Academic, 540 pp.

Robertson, P. K., 1998: Applications Guide - CPT. 1 pp.

Robertson, P. K., R. G. Campanella, D. Gillespie, and J. Greig, 1986: USE OF PIEZOMETER CONE DATA. *Use of In Situ Tests in Geotechnical Engineering, Proceedings of In Situ '86.* ASCE (Geotechnical Special Publ n 6), New York, NY, USA, 1263-1280.

Rouhani, S., and ASTM Committee D-18 on Soil and Rock, 1996: *Geostatistics for environmental and geotechnical applications.* Vol. 1283. Astm, 280 pp.